FACTA UNIVERSITATIS
Series: **Mechanical Engineering**
https://doi.org/10.22190/FUME240403024M

Original scientific paper

COMPREHENSIVE EVALUATION OF DIMENSIONAL DEVIATION, FLANK WEAR, SURFACE ROUGHNESS AND MATERIAL REMOVAL RATE IN DRY TURNING OF C45 STEEL

Aleksandar Milosevic[1], Goran Simunovic[2], Zeljko Kanovic[1], Katica Simunovic[2], Zeljko Santosi[1], Mario Sokac[1], Djordje Vukelic[1]

[1]University of Novi Sad, Faculty of Technical Sciences, Serbia
[2]University of Slavonski Brod, Mechanical Engineering Faculty in Slavonski Brod, Croatia

Abstract. *The study investigated the turning of C45 steel in a dry environment. The input parameters that were varied were cutting speed, feed, depth of cut, corner radius and insert type. The experimental investigations were carried out according to a custom experimental design using the D-optimality criterion. The measured output parameters were dimensional deviation, flank wear and surface roughness, while the material removal rate was calculated. A detailed analysis and evaluation of the effects of the input parameters on the output parameters was carried out. The model was diagnosed and appropriate regression equations were established. Based on the obtained regression equations, multi-objective optimisation was performed using particle swarm optimisation. The objective function was to simultaneously minimise dimensional deviation, flank wear and surface roughness and maximise material removal rate. The optimisation was carried out for different weighting coefficients of each output function for different production requirements. The obtained models and optimal values were verified by additional confirmation experiments.*

Key words: *Dry turning, Dimensional deviation, Flank wear, Surface roughness*

1. INTRODUCTION

Turning is a machining operation that can be carried out under dry or wet conditions and using alternative techniques such as minimum coolant and lubricant quantities, cryogenic cooling, etc. [1,2]. All previous methods of cooling and lubrication have their advantages and disadvantages. The main problems with dry turning are short tool life and

Received: April 03, 2024 / Accepted May 12, 2024
Corresponding author: Goran Simunovic
University of Slavonski Brod, Mechanical Engineering Faculty in Slavonski Brod, Trg Ivane Brlic Mazuranic 2, Slavonski Brod, Croatia
E-mail: gsimunovic@unisb.hr

poor surface quality [3]. Dry turning is associated with high temperatures and is therefore not suitable for machining difficult-to-cut materials [4]. The positive aspects of dry turning are that no cooling lubricant is used and it is therefore environmentally friendly. There are also no additional costs for cutting fluid, equipment, disposal, recycling, reuse, etc. Therefore, dry turning can be used when the materials are characterized by good machinability but the problems mentioned above need to be solved. This can be achieved through the use of stable machines, reliable locating and clamping, the use of coated inserts and, of course, the obligatory optimisation of all the machining parameters entered [5]. C45 steel is a medium carbon steel with a wide range of industrial applications. It is used for the manufacture of various products such as gears, shafts, axles, equipment, tools, etc. It can be used for the manufacture of complex products that need to be machined with high accuracy and precision. It is characterized by good hardness and wear resistance as well as high tensile strength, which makes it the ideal choice for products that need to withstand strong forces. It is not resistant to moisture and aggressive chemicals, so it has low corrosion resistance. It has good machinability when turned, i.e. it does not belong to the group of difficult-to-machine materials and can therefore be turned economically under certain conditions, even in dry conditions.

In the previous period, a large number of researches dealt with the process of turning C45 steel workpieces. Grzesik [6] proposed analytical models for estimating the average and maximum temperatures at the tool–chip interface. The models for a three-layer coating agreed well with both the experimental data and the finite element (FE) predictions. Piska et al. [7] presented wear morphology. The decohesion between the phases and the different size of the phases led to a weakening of the structural integrity, rapid wear of the coating and a short tool life. Stachurski et al. [8] evaluated the influence of cutting parameters on surface roughness. Wiper inserts led to a reduction in surface roughness. Increasing the feed and corner radius contributed to an increase in surface roughness and cutting force. Nieslony et al. [9] presented the influence of constitutive model parameters on the results of FEM-based modelling. A sensitivity analysis of the material flow stress in the power constitutive model was performed. Sergeto et al. [10] used several digital signals from sensor monitoring to identify and monitor the chip shape. Different neural network training algorithms were compared as a decision support system. Michal et al. [11] investigated the influence of cutting speed, feed and depth of cut on surface roughness using regression analysis. The results showed that feed and cutting speed had a dominant influence on surface roughness. Selvam and Senthil [12] studied and optimised the effect of corner radius and turning parameters on surface roughness using the Taguchi method and genetic algorithm. Corner radius had a greater influence on the surface roughness followed by feed and spindle speed and depth of cut. Horvath and Lukacs [13] determined prediction models for estimating the cutting force components based on the undeformed chip cross-section. The results showed that the influence of the effective length of the tool cutting edge on specific cutting force components is not negligible. Necpal et al. [14] compared experimentally determined cutting forces and those predicted by FE simulation. Stress and temperature predictions were made for certain values of cutting speed, feed and depth of cut. Vereschaka et al. [15] investigated the mechanisms of the formation of longitudinal cracks and delamination in coatings on rake and flank surfaces. The properties of the coatings and the nature of their failures were presented. Vereschaka et al. [16] investigated two multilayer nanostructured coatings with the same thickness, elemental composition and basic mechanical properties but different sub-nanolayer thicknesses. A coating with

thicker sub-nanolayers was more prone to delamination. A tool with a coating characterized by a thinner sub-nanolayer thickness had the longest tool life. Klocke et al. [17] developed mathematical relationships considering strain hardening, dynamic forces and shear strain rate. The external and internal friction during the chip formation process was analysed. Dragicevic et al. [18] presented an application of a combined Taguchi and fuzzy logic approach for the optimisation and analysis of surface roughness. Feed and cutting speed were the main parameters influencing the variation of surface roughness. Gjelaj et al. [19] optimised cutting speed, feed, depth of cut as a function of tool path length and cutting force using a genetic algorithm. Zmarzły [20] analysed the influence of feed and cutting speed on surface roughness, roundness and cylindricity. Increasing the feed causes an increase in the deviation of cylindricity. The cutting speed had a negligible effect on the shape of the cylindrical workpieces. Zajac et al. [21] focused on predicting the durability of cutting materials using the Taylor model. Optimal cutting speeds were determined in order to achieve maximum tool life. Usman et al. [22] investigated the effects of cutting speed, feed, depth of cut and ultrasonic vibration amplitude on surface properties using surface function indices. The results showed that the surface function indices obtained in vibration-assisted turning were significantly higher than those obtained in conventional turning. Mikołajczyk [23] presented the investigation of the minimal uncut chip thickness. The main cutting edge angle had a significant influence on the process, especially in the range of small uncut chip thickness range. Titu et al. [24] simulated the effect of rake and clearance angles on temperature distribution, effective stresses and cutting forces using FE analysis. Oleksik et al. [25] analysed vibrations using Fourier transform methods. The influence of vibrations on surface roughness was investigated for two design variants of cutting tools. Abidi [26] investigated the flank wear of ceramic cutting tools as a function of cutting speed and feed. The results show that the flank wear was more strongly influenced by the cutting speed than by the feed. Zaida et al. [27] proposed a method for monitoring flank wear based on the analysis of vibration signals. The method enables estimation of flank wear based on the wavelet transform. Ivchenko et al. [28] developed a method for determining the intensity of tool wear by analysing the cutting edge to determine the change in forces. The method was developed based on a simulation of the machining process, taking into account the tribological interaction of the tool and workpieces as well as the corner radius. Kovalčík et al. [29] proposed a mathematical cutting force model based on the cutting speed and the coating correction factor as well as the cutting edge geometry. Jurko et al. [30] performed optimisation of flank wear and diameter deviation by using Grey Relation Analysis (GRA) in combination with the Taguchi method. Cutting speed was an important factor influencing the multiple responses on the effect of insert wear on average diameter deviation. Vukelic et al. [31] modelled surface roughness in finish turning as a function of corner radius, approach angle, rake angle and inclination angle. The surface roughness improved with increasing corner radius, increasing approach angle, increasing rake angle and decreasing inclination angle. Niemczewska-Wojcik et al. [32] focused on the surface topography of workpieces under dry and wet conditions. The mineral oil-based lubricant had a positive influence on tool wear and surface quality. Kuruc et al. [33] analysed the plastic deformation and chip compression. Plastic deformation decreased with increasing feed and cutting speed. Chip compression decreased with increasing cutting speed. Moravčíková et al. [34] presented the influence of the heat treatment (soft annealing, normalisation, hardening, quenching and tempering) of C45 steel on roughness, cylindricity and circularity. The heat treatment

had a major influence on all output parameters. Slusarczyk and Franczyk [35] presented a method for determining the feed and tangential components of the cutting force. The method was based on the assumptions that the tool is perfectly sharp, that the chip formation process is continuous, that the chip thickness is constant and that there are no heat losses.

In general, the main disadvantage of experimental research is the high time expenditure and the associated costs, therefore the modelling of the turning process and its optimisation is an increasing topic. In previous research, the most common input parameters were cutting speed, feed rate, depth of cut, geometric parameters of the cutting tool, type of coating, etc., while the most common output parameters were surface roughness, wear mechanisms of the cutting tool, cutting forces, tool life, material removal rate, etc. In order to reduce the number of experiments and significantly reduce costs, modelling and optimisation are carried out. The problem with modelling and optimisation is the choice of method, as there are no universal and generally accepted rules. Only confirmation of unknown values of input parameters and comparison with measured values can influence the validity of the applied modelling and optimisation method. If the process is modelled and optimised correctly and acceptable errors are achieved, costs and time are reduced. The general validity and independence of the results from the knowledge and experience of the technologists is also greater.

In contrast to the previous work, this study shows the influence of a larger number of input parameters on a larger number of output parameters in dry turning of C45 steel. So far, the comprehensive evaluation of the influence of cutting speed, feed, depth of cut, corner radius and insert type on surface roughness, dimensional deviation, flank wear and the material removal rate has not been performed. The influence of the interactions of the input parameters on the output parameters was also investigated. A detailed analysis of the input parameters and an evaluation of their effect on the output parameters of the process were carried out. In addition, the modelling and optimisation of the process and the verification of the solutions obtained were carried out.

2. RESEARCH METHODOLOGY

The research methodology is shown in Fig. 1. The tests were carried out on samples of C45 steel with the following properties: Young's modulus 205 GPa, hardness 255, tensile strength 560 MPa and density 7.85 g/cm^3. The chemical composition of the steel is as follows: 0.42–0.50 % C, max 0.40 % Si, 0.50–0.80 % Mn, max 0.40 % Ni, max 0.030 % P, max 0.035 % S, max 0.40 % Cr and max 0.10 % Mo.

Dry turning was carried out on a CNC lathe. A three-jaw chuck and rotary centre were used for locating and clamping. Based on the recommendations of the cutting insert manufacturer and in accordance with the characteristics of the workpiece material, the geometry of the workpiece, the type of sequence, the characteristics of the technological equipment and stability, the machining parameters and the cutting inserts were selected. Both types of inserts (standard and wiper) with the following characteristics were used for the study: rhombic shape (80°), thickness 4.8 mm, diameter of the inscribed circle 12.7 mm, effective length of the cutting edge 11.7 mm and fixing hole 5.2 mm. The inserts were coated using CVD coating technology (TiCN+Al_2O_3+TiN coating of 5 μm thickness). The

turning parameters were as follows: cutting speed v_c = 300–400 (mm/min), feed f = 0.1–0.25 (mm/rev) and depth of cut a_p = 2–3 (mm).

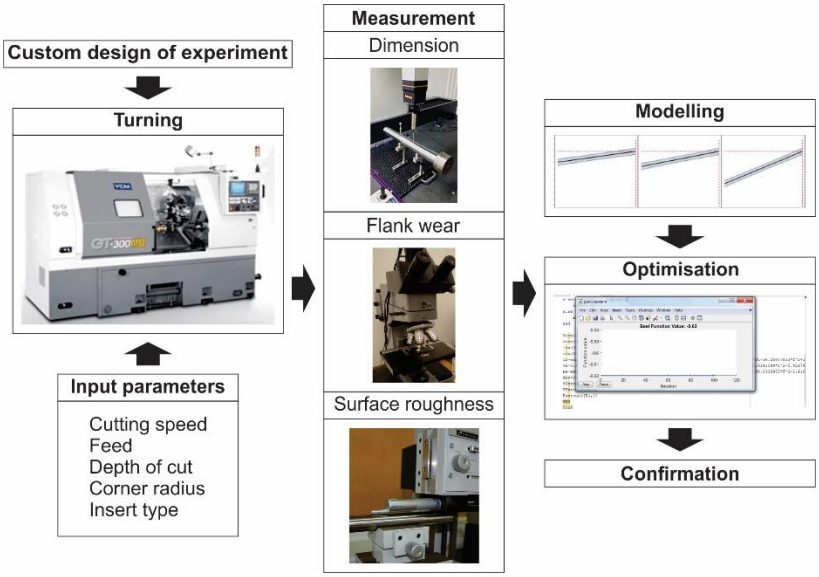

Fig. 1 Research methodology

After the experimental investigation, the output parameters were measured and calculated. The measurements of dimensions, surface roughness and flank wear were carried out under controlled microclimatic conditions. The measured output parameters were dimensional deviation (ΔD), surface roughness (Ra) and flank wear (VB) while the material removal rate (MRR) was calculated.

The surface roughness was measured using a Talysurf measuring device. The measurements were taken in the feed direction with a sampling length of 0.8 mm and an evaluation length of 4 mm using a Gaussian filter.

The diameter of the workpiece before and after turning was measured using a CRYSTA-Apex S 9106 coordinate measuring machine, resolution 0.0001 mm and accuracy of 1.7 + measuring length/1000 μm, with a probe in the form of a ruby ball with a diameter of 5 mm. The large diameter of the probe was chosen to reduce the influence of surface roughness on the relative error of the diameter change. The diameter change represents the difference between the nominal diameter and the measured diameter of the machined surface.

The measurement of flank wear was carried out with a Leitz Orthoplan light optical microscope using the ImageJ software.

The fourth output parameter, the material removal rate, was calculated using the equation:

$$MRR = v_c \cdot a_p \cdot f \tag{1}$$

After measurement and calculation, the process was analysed and modelled. The experimental investigations were carried out according to the custom experimental design,

which enables the creation of an optimal experimental design with a lower number of trials (minimising costs) and the achievement of reliable and relevant results. The customised experimental design was created using the D-optimal criterion. The experimental design was determined based on the previously defined input and output parameters. In determining the experimental design, an a priori model was defined that includes main effects, their quadratic effects and two-factor interactions as expected influences of the input parameters on the output parameters. The number of experimental points was chosen depending on the complexity of the process and the desire for an accurate estimation of the output parameters of the model. In evaluating the experimental design, it was determined that 72 trials had sufficient statistical power to determine the effects of the input parameters. The experimental design was randomised to eliminate system bias and ensure the reliability of the results.

After modelling phase, a multi-objective optimisation was conducted using particle swarm optimisation (PSO) algorithm. PSO is a global optimisation algorithm suitable for multi-objective optimum search. It is based on behaviour imitation of living beings moving in groups (swarms, flocks, …) and operates with the set of individuals (particles), called swarm. In simple words, particles are moving throughout the search space searching for the point that achieves the best value of objective function. The search is iterative, and is conducted until the defined stopping criterion is fulfilled. Each particle in the swarm is defined by its "position" **y**, which represents the vector of variables in the optimisation problem, or „coordinates" in the search space, and by its current "velocity" **v**. In other words, particle's position is the potential solution of the optimisation problem, containing the values of variables, and the velocity determines the way of modification of these values in order to obtain global optimum. In this study, the position of the particle (vector **y**) is defined by values of input parameters, namely cutting speed v_c, depth of cut a_p, feed f and corner radius r. Also, during the search process, each particle is capable of memorizing its "personal" best position **p**, as well as the "global" best position **g** achieved by the entire swarm, which is the information "shared" between all particles. The particle is basically guided by three velocity components: inertia (forces the particle to move in the same direction as in previous iteration), cognitive component (the particle is motivated by its personal experience and guided by its personal best position **p**), and social component (guides the particle according to global knowledge of the swarm, i.e. towards the global best position **g**). Accordingly, the particle's position is updated using the following expression:

$$\mathbf{v}^{(k+1)} = w \cdot \mathbf{v}^{(k)} + cp \cdot rp^{(k)} \cdot \left(\mathbf{p}^{(k)} - \mathbf{y}^{(k)}\right) + cg \cdot rg^{(k)} \cdot \left(\mathbf{g}^{(k)} - \mathbf{y}^{(k)}\right) \tag{2}$$

$$\mathbf{y}^{(k+1)} = \mathbf{y}^{(k)} + \mathbf{v}^{(k+1)} \tag{3}$$

where k is the number of the current iteration, factors w, cp and cg determine the influence of inertial, cognitive and social components respectively, and factors rp and rg are random numbers uniformly distributed in range [0,1], providing the stochastic nature of the algorithm. In each iteration, personal best position **p** and global best position **g** are updated according to the values of objective function. The initial positions of particles are chosen randomly, within the boundaries of the search space. The initial velocities are either set to zero or chosen randomly, depending on the variant of the algorithm. The iterative process is repeated until the specified stopping criterion is fulfilled, which is mainly the total number of iterations or, alternatively, the number of successive iterations in which the value of objective function does not change (stalls).

Finally, the models, regression equations and optimum values of the input and output parameters were validated by additional confirmation tests.

3. RESULTS

3.1 Experimental Research

The D-optimality criterion was used for the experimental design, as it ensures an accurate estimation of the effects of the input parameters. The optimum number of experimental points was selected by analysing experimental designs with different numbers of trials. The comparison was carried out using the compare designs function for designs with 32, 48, 64, 72 and 96 experimental points. The minimum number of experimental points required, the performance and characteristics of experimental designs as well as the availability of resources, time and costs of experiment execution were then taken into account using the power analysis. The power analysis makes it possible to determine the ability of the experiment to recognise real effects, i.e. to identify the existence of effects. In the power analysis, the following reference values were defined for evaluating the power of the model: significance level 0.05 and anticipated root mean square error (RMSE) 1. The obtained evaluation parameters of different experimental designs (ranging from 0 to 1 and referring to the main effects, their quadratic effects and two-factor interactions) show that the experimental designs for 72 and 96 trials have the statistical power to detect real effects (Fig. 2).

Power Analysis

Significance Level 0.05

Anticipated RMSE 1

Term	Anticipated Coefficient	Exp. 2 - 32 Power	Exp. 2 - 48 Power	Exp. 2 - 64 Power	Exp. 2 - 72 Power	Exp. 2 - 96 Power
Intercept	1	0.278	0.417	0.546	0.655	0.771
v	1	0.995	1.000	1.000	1.000	1.000
v*v	1	0.419	0.582	0.762	0.831	0.903
a	1	0.999	1.000	1.000	1.000	1.000
f	1	0.996	1.000	1.000	1.000	1.000
f*f	1	0.383	0.637	0.808	0.845	0.956
r	1	0.996	1.000	1.000	1.000	1.000
r*r	1	0.383	0.639	0.829	0.846	0.956
Insert	1	0.999	1.000	1.000	1.000	1.000
v*a	1	0.997	1.000	1.000	1.000	1.000
v*f	1	0.992	1.000	1.000	1.000	1.000
v*r	1	0.992	1.000	1.000	1.000	1.000
v*Insert	1	0.997	1.000	1.000	1.000	1.000
a*f	1	0.997	1.000	1.000	1.000	1.000
a*r	1	0.997	1.000	1.000	1.000	1.000
a*Insert	1	0.999	1.000	1.000	1.000	1.000
f*r	1	0.991	1.000	1.000	1.000	1.000
f*Insert	1	0.996	1.000	1.000	1.000	1.000
r*Insert	1	0.996	1.000	1.000	1.000	1.000

Good 0.80 0.60 0.40 0.20 Bad

Fig. 2 Power analysis

In view of the small differences in power between these two experimental designs, the design with 72 test points was chosen as it consumes significantly fewer resources. Of the total 72 trials, 63 are different trial points and 9 are replicates.

The selected levels of the input parameters are listed in Table 1.

Table 1 Input parameters and the selected levels

Input parameter	Level 1 (Minimum)	Level 2 (Middle)	Level 3 (Middle)	Level 4 (Maximum)
Cutting speed v_c (mm/min)	300	350	/	400
Feed f (mm/rev)	0.1	0.15	0.2	0.25
Depth of cut a_p (mm)	2	/	/	3
Corner radius r (mm)	0.4	0.8	1.2	1.6
Insert type	Standard	/	/	Wiper

The results of the measurement and calculation of the output parameters is shown in Table 2.

Table 2 Results of experiments

No.	v_c (mm/min)	a_p (mm)	f (mm/rev)	r (mm)	*Insert type*	ΔD (mm)	*VB* (mm)	*Ra* (μm)	*MRR* (mm^3/min)
1	300	2	0.2	1.2	Wiper	0.054	0.102	0.659	120
2	300	3	0.25	1.6	Standard	0.111	0.130	2.768	225
3	300	2	0.25	1.6	Wiper	0.106	0.097	1.294	150
4	400	3	0.25	0.4	Standard	0.289	0.211	7.236	300
5	400	3	0.15	0.8	Standard	0.052	0.184	1.303	180
6	400	2	0.25	1.6	Wiper	0.111	0.141	1.354	200
7	300	3	0.1	1.6	Wiper	0.017	0.090	0.210	90
8	350	2	0.2	0.4	Standard	0.178	0.162	4.449	140
9	300	2	0.1	1.6	Standard	0.017	0.111	0.435	60
10	300	2	0.15	1.6	Standard	0.039	0.115	0.978	90
11	400	3	0.2	1.6	Standard	0.074	0.170	1.853	240
12	300	2	0.25	1.6	Standard	0.109	0.123	2.717	150
13	300	2	0.1	0.8	Standard	0.022	0.129	0.543	60
14	400	3	0.25	0.4	Standard	0.291	0.213	7.237	300
15	400	2	0.25	0.4	Standard	0.284	0.205	7.109	200
16	400	3	0.25	1.6	Wiper	0.112	0.147	1.379	300
17	400	3	0.1	0.4	Wiper	0.045	0.172	0.643	120
18	400	3	0.2	0.4	Wiper	0.182	0.180	2.573	240
19	300	3	0.1	1.6	Standard	0.019	0.118	0.442	90
20	300	2	0.25	0.4	Wiper	0.266	0.134	3.773	150
21	400	2	0.1	0.4	Standard	0.046	0.192	1.138	80
22	300	3	0.15	1.2	Wiper	0.031	0.104	0.377	135
23	400	3	0.25	0.4	Wiper	0.284	0.184	4.020	300
24	300	2	0.1	1.6	Wiper	0.017	0.084	0.207	60
25	400	3	0.1	1.2	Standard	0.015	0.171	0.386	120
26	350	2	0.25	1.2	Standard	0.093	0.141	2.317	175
27	300	2	0.25	0.4	Standard	0.272	0.160	6.792	150
28	400	2	0.25	0.4	Wiper	0.279	0.178	3.950	200
29	300	2	0.1	0.4	Standard	0.040	0.148	1.087	60
30	300	3	0.2	0.4	Wiper	0.174	0.136	2.460	180
31	350	2	0.1	1.2	Standard	0.015	0.129	0.371	70

32	350	3	0.25	1.6	Wiper	0.111	0.114	1.348	262.5
33	400	2	0.25	1.6	Standard	0.114	0.168	2.844	200
34	400	2	0.15	0.4	Wiper	0.100	0.170	1.422	120
35	400	2	0.1	1.2	Wiper	0.014	0.138	0.172	80
36	300	3	0.25	0.4	Standard	0.277	0.167	6.919	225
37	350	3	0.25	0.8	Standard	0.142	0.155	3.539	262
38	300	3	0.1	0.4	Standard	0.044	0.154	1.107	90
39	300	3	0.1	0.4	Standard	0.043	0.153	1.106	90
40	300	3	0.2	1.2	Standard	0.059	0.135	1.476	180
41	400	2	0.1	0.4	Wiper	0.045	0.165	0.632	80
42	300	3	0.1	0.4	Wiper	0.043	0.127	0.615	90
43	400	2	0.2	0.8	Standard	0.091	0.182	2.275	160
44	300	3	0.25	1.6	Wiper	0.108	0.103	1.318	225
45	350	2	0.25	0.4	Wiper	0.273	0.142	3.862	175
46	350	2	0.15	0.8	Wiper	0.048	0.117	0.624	105
47	400	3	0.25	1.2	Wiper	0.091	0.157	1.096	300
48	300	3	0.25	1.6	Standard	0.112	0.131	2.766	225
49	400	2	0.25	1.6	Standard	0.115	0.169	2.843	200
50	400	3	0.1	0.8	Wiper	0.022	0.153	0.289	120
51	400	2	0.15	1.6	Standard	0.041	0.159	1.024	120
52	400	3	0.1	1.6	Standard	0.019	0.161	0.463	120
53	350	2	0.2	1.6	Wiper	0.070	0.104	0.848	140
54	350	3	0.1	1.6	Standard	0.019	0.126	0.453	105
55	400	3	0.25	1.6	Standard	0.116	0.174	2.895	300
56	400	3	0.1	1.6	Wiper	0.018	0.135	0.221	120
57	400	2	0.1	1.6	Wiper	0.018	0.128	0.217	80
58	400	2	0.25	0.8	Wiper	0.137	0.160	1.777	200
59	400	3	0.1	0.4	Standard	0.044	0.196	1.157	120
60	400	2	0.1	1.6	Wiper	0.017	0.126	0.216	80
61	350	3	0.15	0.4	Standard	0.102	0.164	2.548	157.5
62	300	2	0.1	0.4	Wiper	0.043	0.121	0.604	60
63	300	2	0.1	0.4	Wiper	0.042	0.119	0.602	60
64	300	2	0.25	0.4	Standard	0.271	0.158	6.790	150
65	350	3	0.1	0.4	Wiper	0.044	0.136	0.629	105
66	400	3	0.15	1.6	Wiper	0.041	0.139	0.496	180
67	300	2	0.25	1.6	Wiper	0.108	0.099	1.292	150
68	400	2	0.1	1.6	Standard	0.018	0.155	0.455	80
69	300	3	0.25	0.4	Wiper	0.271	0.140	3.844	225
70	400	2	0.1	0.4	Standard	0.047	0.193	1.140	80
71	300	3	0.1	1.6	Wiper	0.019	0.091	0.212	90
72	300	3	0.25	0.8	Wiper	0.133	0.121	1.730	225

3.2 Process Analysis and Modelling

The statistical analysis of the experimental results was carried out using SAS JMP 14 software. The statistical analysis was performed separately for each output parameter in order to better interpret the results and determine the specific effects of each input parameter. In the statistical analysis, a model was chosen that includes main effects, their quadratic effects and two-factor interactions. The selected regression model consists of 20 terms and defines the variances of ΔD, *VB* and *Ra* using the minimum number of required variations. Given the irregularities in the distribution of the data and the excessive deviations between the values, a logarithmic transformation (ln) of ΔD and *Ra* was performed to facilitate the application and interpretation of the statistical method.

Fig. 3 shows the evaluation of the quality of the fitting the regression models to the experimental data (actual) by comparing the dependence of the actual on the predicted output parameters. The resulting plots show a good predictive power of the model as the data points follow a diagonal line, which is an ideal arrangement when the actual output parameters are identical to the predicted output parameters. The proximity of the points to the diagonal indicates a narrow confidence interval, i.e. a high degree of accuracy in the model predictions.

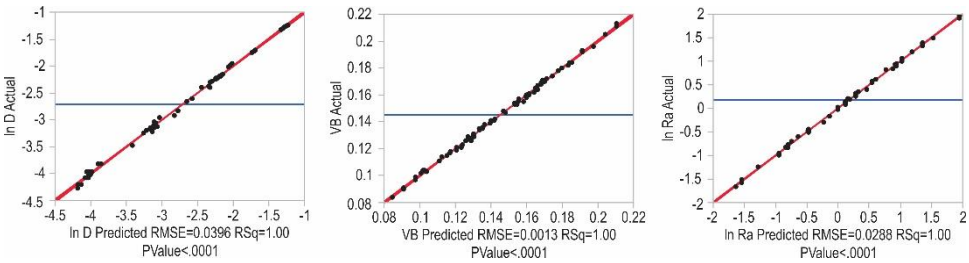

Fig. 3 Actual by predicted plot

Table 3 shows a summary of the fit, which provides key statistical data on the quality of the selected regression models for each output parameter. The coefficient of determination (RSquare) values for all output parameters are close to 1, indicating a high degree of fit between the model and the data. The coefficients of determination mean that more than 99% of the variability of the responses is explained by the specified input parameters. The difference between the values of RSquare and RSquare Adj is small, which means that additional parameters in the model do not contribute to improving the explanation of variability. Low values of RMSE (0.039579, 0.001286 and 0.028794) indicate that the difference between the actual and predicted values is low.

Table 3 Summary of fit

Parameter	ln ΔD	VB	ln Ra
RSquare	0.998399	0.998371	0.999257
RSquare Adj	0.998224	0.998193	0.999188
Root mean square error	0.039579	0.001286	0.028794
Mean of response	-2.71538	0.145361	0.181747

Table 4 shows the analysis of variance of the regression models, which provides an assessment of the effectiveness of the selected models in explaining the variability of the data. Low values of Prob>F (<0.0001) suggest that the models are significant, i.e., there is a real influence of input parameters, that is, they indicate the presence of at least one significant effect in the model.

Table 5 shows the lack of fit of the model to the data. Since the Prob>F values for all three output parameters are greater than 0.05, it can be concluded that there is no statistically significant lack of fit. In other words, the models fit the data well and there is no need for further adjustments.

Table 4 Analysis of variance

Output parameter	Source	DF	Sum of Squares	Mean Square	F Ratio	Prob > F
ln Δ*D*	Model	7	62.538877	8.93413	5703.154	<.0001
	Error	64	0.100258	0.00157		
	C. Total	71	62.639134			
VB	Model	7	0.06487678	0.009268	5604.625	<.0001
	Error	64	0.00010583	$1.654 \cdot 10^{-6}$		
	C. Total	71	0.06498261			
ln *Ra*	Model	6	72.433757	12.0723	14561.24	<.0001
	Error	65	0.053890	0.000829		
	C. Total	71	72.487647			

Table 5 Lack of fit

Output parameter	Source	DF	Sum of Squares	Mean Square	F Ratio	Prob > F	Max RSq
ln Δ*D*	Lack of Fit	54	0.09138242	0.001692	1.9068	0.1346	0.9999
	Pure Error	10	0.00887509	0.000888			
	Total Error	64	0.10025751				
VB	Lack of Fit	54	0.00009333	1.7284e-6	1.3827	0.3008	0.9998
	Pure Error	10	0.00001250	1.25e-6			
	Total Error	64	0.00010583				
ln *Ra*	Lack of Fit	23	0.02598929	0.001130	1.7010	0.0665	0.9996
	Pure Error	42	0.02790028	0.000664			
	Total Error	65	0.05388956				

Table 6 shows the summary of effects of the model sorted by statistical significance for each output parameter. High Log Worth values indicate a larger effect. Regarding the regression model for dimensional deviation, the P-values indicate that the linear effects of all input parameters and the quadratic effects of corner radius and feed are significant, while the interaction terms are not significant. Statistically significant terms for flank wear are the linear effects of all input parameters and the quadratic effects of cutting speed and corner radius. For surface roughness, the main effects of feed, corner radius and insert type, the quadratic effects of corner radius and feed and the interaction of the corner radius with insert type are statistically significant.

Table 6 Effect summary

Source	ln Δ*D* Log Worth	P Value	Source	*VB* Log Worth	P Value	Source	ln *Ra* Log Worth	P Value
f(0.1,0.25)	86.957	0.00000	v_c(300,400)	79.370	0.00000	*f*(0.1,0.25)	96.952	0.00000
r(0.4,1.6)	67.751	0.00000	*r*(0.4,1.6)	72.975	0.00000	*r*(0.4,1.6)	79.872	0.00000
r×*r*	46.141	0.00000	*Insert*	67.429	0.00000	*Insert*	71.682	0.00000
f×*f*	23.093	0.00000	*f*(0.1,0.25)	45.031	0.00000	*r*×*r*	55.108	0.00000
v_c(300,400)	4.785	0.00002	$v_c \times v_c$	40.134	0.00000	*f*×*f*	32.008	0.00000
Insert	2.498	0.00318	a_p(2,3)	29.385	0.00000	*r*×*Insert*	13.908	0.00000
a_p(2,3)	1.699	0.02002	*r*×*r*	17.689	0.00000			

The least squares estimates of the regression coefficients in regression models for each output parameter are shown in Table 7. The P-value (Prob>|t|) is a statistical measure that indicates whether the regression coefficient is statistically significant. Regression coefficients for which the P-value is less than 0.05 (at a significance level of 0.05) are statistically significant, which means that they have a measurable influence on the output parameters. Based on the t-test for each regression coefficient, it can be concluded from Table 7 that all regression coefficients make a significant contribution to the model for each output parameter.

Table 7 Parameter estimates

Output parameter	Term	Parameter Estimate	Std. Error	t Ratio	Prob>|t|
	Intercept	-4.248929915	0.01394	-212.63	<.0001
	v_c(300,400)	0.0004741868	0.005086	4.66	<.0001
	a_p(2,3)	0.0222581906	0.004665	2.39	0.0200
	f(0.1,0.25)	24.923894213	0.00521	176.07	<.0001
ln ΔD	f×f	-36.26807853	0.012883	-15.84	<.0001
	r(0.4,1.6)	-3.61217157	0.005208	-87.96	<.0001
	r×r	1.4243724919	0.012883	39.80	<.0001
	Insert [Standard]	0.01430008923	0.004665	3.07	0.0032
	Insert [Wiper]	-0.01430008923	0.004665	-3.07	0.0032
	Intercept	0.6515022469	0.000479	268.80	<.0001
	v_c(300,400)	-0.003352888	0.000165	133.91	<.0001
	v_c×v_c	5.421798 10-6	0.000427	31.72	<.0001
	a_p(2,3)	0.0062934453	0.000152	20.74	<.0001
VB	f(0.1,0.25)	0.0862505098	0.000169	38.18	<.0001
	r(0.4,1.6)	-0.058217909	0.000169	-106.28	<.0001
	r×r	0.0141088	0.000415	12.24	<.0001
	Insert [Standard]	0.0131866107	0.000152	86.93	<.0001
	Insert [Wiper]	-0.0131866107	0.000152	-86.93	<.0001
	Intercept	-1.109854932	0.010118	-5.34	<.0001
	f(0.1,0.25)	25.493860539	0.003788	241.16	<.0001
	f×f	-38.0339955	0.009377	-22.82	<.0001
	r(0.4,1.6)	-3.651190406	0.003788	-131.51	<.0001
ln *Ra*	r×r	1.4103920332	0.009365	54.21	<.0001
	Insert [Standard]	0.3334098556	0.003393	98.25	<.0001
	Insert [Wiper]	-0.3334098556	0.003393	-98.25	<.0001
	r×*Insert* [Standard]	0.0376169575	0.003793	9.92	<.0001
	r×*Insert* [Wiper]	-0.0376169575	0.003793	-9.92	<.0001

Fig. 4 shows that the residuals are randomly distributed along the horizontal axis (row number, according to Table 2) for each output parameter, indicating no trend or systematic irregularities in the distribution of the residuals.

Fig. 5 shows the normal quantile plots of the residuals. The residual normal quantile plots allow an assessment of the normality of the residuals in the model. The distribution of the points on the plots follows the diagonals and the points are not outside the range, which indicates a normal distribution of the residuals.

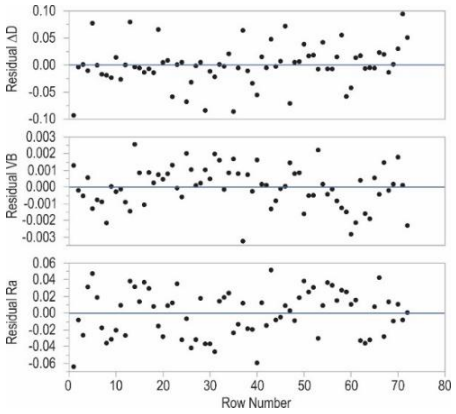

Fig. 4 Residual by row plot

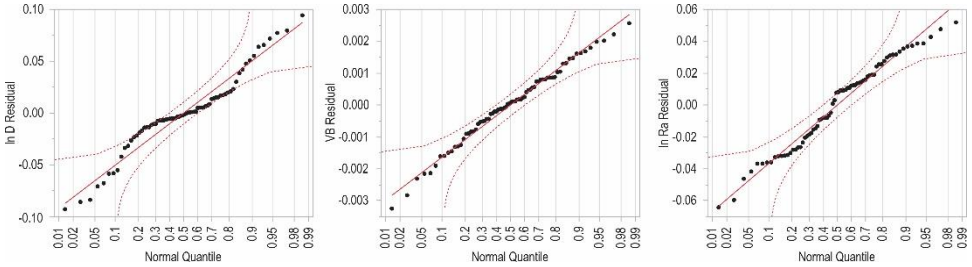

Fig. 5 Residual normal quantile plot

Statistical analysis of the data for the selected models yields the following regression equations for dimensional deviation, flank wear and surface roughness, respectively:

$$\ln \Delta D = -4.248929915 + 0.0222581906 \cdot a_p + 24.923894213 \cdot f - 3.61217157 \cdot r + 0.0004741868 \cdot v_c - 36.26807853 \cdot f^2 + 1.4243724919 \cdot r^2 + Match\,(Insert)\begin{pmatrix} "Standard" & \Rightarrow & 0.01430008923 \\ "Wiper" & \Rightarrow & -0.01430008923 \\ else & \Rightarrow & . \end{pmatrix} \quad (4)$$

$$VB = 0.6515022469 + 0.0062934453 \cdot a_p + 0.0862505098 \cdot f - 0.058217909 \cdot r - 0.003352888 \cdot v_c + 0.0141088 \cdot r^2 + 5.421798 \cdot 10^{-6} \cdot v_c^2 + Match(Insert)\begin{pmatrix} "Standard" & \Rightarrow & 0.0131866107 \\ "Wiper" & \Rightarrow & -0.0131866107 \\ else & \Rightarrow & . \end{pmatrix} \quad (5)$$

$$\ln Ra = -1.109854932 + 25.493860539 \cdot f - 3.651190406 \cdot r - 1.666666667 \cdot Match(Insert)\begin{pmatrix} "Standard" & \Rightarrow & 0.0376169575 \\ "Wiper" & \Rightarrow & -0.0376169575 \\ else & \Rightarrow & . \end{pmatrix} - 38.0339955 \cdot f^2 + 1.4103920332 \cdot r^2 + 1.666666667 \cdot r \cdot Match(Insert)\begin{pmatrix} "Standard" & \Rightarrow & 0.0376169575 \\ "Wiper" & \Rightarrow & -0.0376169575 \\ else & \Rightarrow & . \end{pmatrix} + Match(Insert)\begin{pmatrix} "Standard" & \Rightarrow & 0.3334098556 \\ "Wiper" & \Rightarrow & -0.3334098556 \\ else & \Rightarrow & . \end{pmatrix} \quad (6)$$

For the surface roughness, Fig. 6 shows a statistically significant interaction between the corner radius and the insert type. The influence of the interaction is most pronounced for the smallest corner radius (r=0.4 mm) and for the standard insert. The influence of the interaction is lowest for the corner radius r=1.2 mm and for the wiper insert.

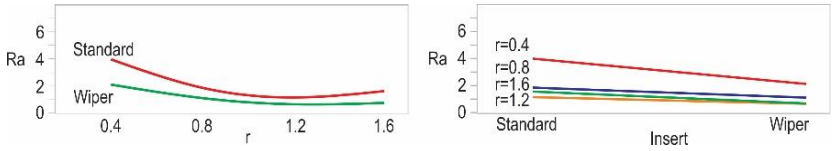

Fig. 6 Interaction profiles

The prediction profilers shown in Fig. 7 visually display the optimal values for each output parameter as a function of each input parameter.

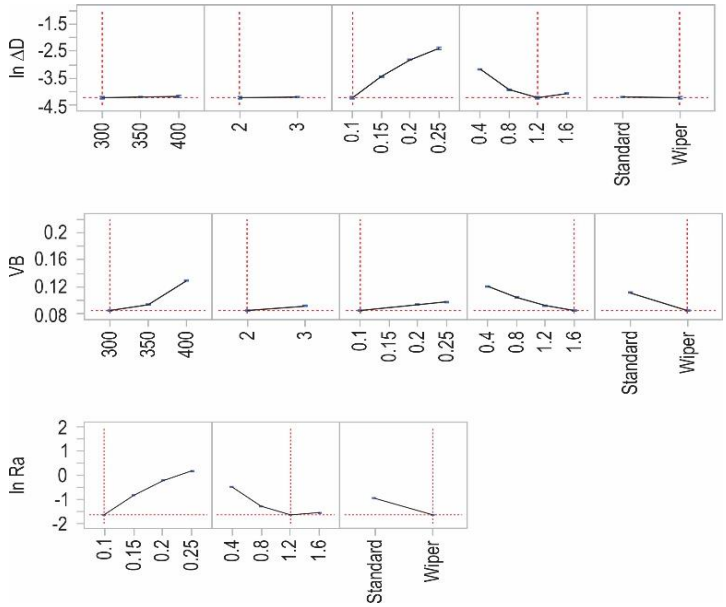

Fig. 7 Prediction profiler

As shown in Fig. 7, the minimum value of the dimensional deviation (ΔD=0.014 mm) is achieved at the minimum value of the cutting speed (v_c=300 mm/min), the minimum value of the depth of cut (a_p=2 mm), the minimum value of the feed (f=0.1 mm/rev), the value of corner radius r=1.2 mm and for the wiper insert. The minimum value of the flank wear (VB=0.084 mm) is achieved at the minimum value of the cutting speed (v_c=300 mm/min), the minimum value of the depth of cut (a_p=2 mm), the minimum value of the feed (f=0.1 mm/rev), the maximum value of the corner radius (r=1.6 mm) and for the wiper insert. The minimum value of the surface roughness (Ra=0.172 μm) is achieved at the minimum feed value (f=0.1 mm/rev), the value of corner radius r=1.2 mm and for the wiper cutting insert and does not depend on the cutting speed and the depth of cut. The maximum

value of the material removal rate (*MRR*=300 mm^3/min) was achieved at the maximum value of the cutting speed (v_c=400 mm/min), feed (f=0.25 mm/rev) and depth of cut (a_p=3 mm) and does not depend on the corner radius and insert type.

Given the conflicting requirements of the individual objective functions and in order to find a compromise solution for different production conditions and requirements, it is necessary to perform a multi-objective optimisation.

3.3 Process Optimisation

The objective function is defined as follows:

$$F_c = w_{\Delta D} \cdot \min x_{\Delta D} + w_{VB} \cdot \min\ x_{VB} + w_{Ra} \cdot \min x_{Ra} + w_{MRR} \cdot \max\ x_{MRR} \tag{7}$$

where $w_{\Delta D}$, w_{VB}, w_{Ra}, w_{MRR} are weight coefficients determining the significance of each output parameter in objective function, and $x_{\Delta D}$, x_{VB}, x_{Ra}, x_{MRR} are normalized values of output parameters (expression 8). In other words, the problem is defined as multi-objective optimisation seeking for minimum of ΔD, *VB* and *Ra*, and maximum of *MRR*.

In order to eliminate the influence of the absolute values of the output parameters, their values were normalised using the following expressions:

$$x_{Ra} = \frac{Ra - Ra_{min}}{Ra_{max} - Ra_{min}},\ x_{\Delta D} = \frac{\Delta D - \Delta D_{min}}{\Delta D_{max} - \Delta D_{min}},\ x_{VB} = \frac{VB - VB_{min}}{VB_{max} - VB_{min}},\ x_{MRR} = \frac{MRR - MRR_{min}}{MRR_{max} - MRR_{min}} \tag{8}$$

where indices *min* and *max* determine the lowest and highest permitted value of each output parameter. As already mentioned, the "coordinates" of particle's position vector **y** in PSO algorithm are the input parameters v_c, a_p, f and r. Maximum number of iterations was 1000, and as alternative stopping criterion the number of 100 stall generations was used. The recommendations for adopting these values are not strictly defined in the literature, i.e. they depend on the particular optimisation problem. In practice, these values are determined experimentally, using trial and error procedure, which was also applied in this research.

In accordance with experimental research, the following limitations for input parameters were defined:

- $v_{cmin} \le v_{ci} \le v_{cmax}$; $300 \le v_{ci} \le 400\ \forall i \in [1,\ldots,n]$; continuous input parameter,
- $f_{min} \le f_i \le f_{max}$; $0.1 \le f_i \le 0.25\ \forall i \in [1,\ldots,n]$; continuous input parameter,
- $a_{pmin} \le a_{pi} \le a_{pmax}$; $2 \le a_p \le 3\ \forall i \in [1,\ldots,n]$; continuous input parameter,
- $r_{imin} \le r_i \le r_{imax}$; $r_i = 0.4 \vee 0.8 \vee 1.2 \vee 1.6$; categorical input parameter,
- *IT*= Standard ∨ Wiper; categorical input parameter.

The optimisation results for different values of the weighting coefficients are shown in Table 8.

Table 8 Optimisation results

No.	Weighting coefficients				Optimal input parameters				
	$w_{\Delta D}$	w_{VB}	w_{Ra}	w_{MRR}	v_c (mm/min)	a_p (mm)	f (mm/rev)	r (mm)	*Insert type*
1	1	1	1	1	340	3	0.2	1.2	Wiper
2	1	0	1	1	400	3	0.25	1.2	Wiper
3	1	0	1	0	328	2.1	0.1	1.2	Wiper

3.4 Confirmation Experiments

The models obtained were verified by seven additional confirmation experiments. The confirmation experiments were carried out to check the generalisability of the models formed and the validation of the optimal values. The confirmation experiments were carried out both with combinations of input parameters with which the modelling of the turning process was not carried out (experiments 1–4, Table 9) and with combinations of input parameters for which optimal output parameters were determined (experiments 5–7, Table 9). The results obtained for the seven combinations mentioned above are shown in Table 9. The performance evaluation was carried out by calculating the absolute and percentage errors. The graphical interpretation of the obtained minimum, mean and maximum values of the absolute and percentage errors for ΔD, *VB* and *Ra* is shown in Fig. 8.

Table 9 Confirmation experiments results

No.	v_c (mm/min)	a_p (mm)	f (mm/rev)	r (mm)	Insert type	Predicted			Measure		
						ΔD (mm)	*VB* (mm)	*Ra* (μm)	ΔD (mm)	*VB* (mm)	*Ra* (μm)
1	325	2.5	0.125	1.2	Standard	0.023	0.125	0.593	0.024	0.128	0.606
2	325	2.5	0.125	1.2	Wiper	0.022	0.098	0.297	0.023	0.096	0.303
3	375	2.5	0.175	1.2	Standard	0.048	0.151	1.198	0.05	0.154	1.216
4	375	2.5	0.175	1.2	Wiper	0.046	0.125	0.601	0.047	0.129	0.609
5	340	3	0.2	1.2	Wiper	0.062	0.112	0.795	0.063	0.114	0.807
6	328	2.1	0.1	1.2	Wiper	0.015	0.094	0.192	0.016	0.097	0.195
7	400	3	0.25	1.2	Wiper	0.098	0.156	1.191	0.099	0.158	1.207

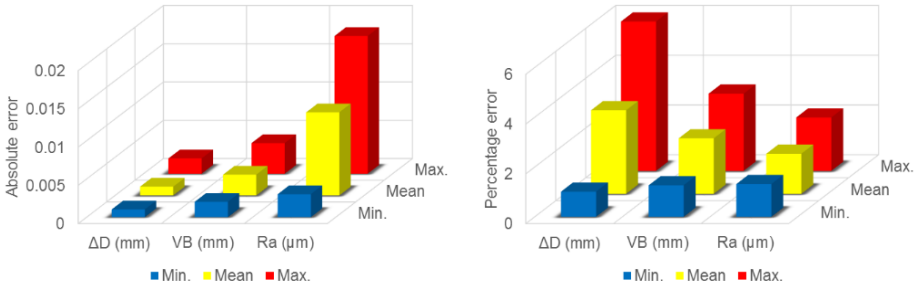

Fig. 8 Absolute and percentage errors

4. DISCUSSION

The results of the experiments, statistical analysis, modelling, optimisation and confirmation showed that the different input parameters have a different influence on the output parameters.

As the cutting speed increases, the flank wear increases. An identical tendency was found in [26], but some of the studies showed the opposite, i.e. that when the cutting speed is decreased, the wear becomes more intense due to the generation of smaller cutting forces [16], but when using multilayer composite nano-structured modified coatings. When the cutting speed increases, the temperature in the machining zone increases, which leads to higher flank wear. The consequence of the higher flank wear is a slight deterioration in the dimensional deviation. It can also be observed that the flank wear has not reached a critical level, so that it does not significantly affect the surface roughness.

As the feed increases, surface roughness and flank wear increase. A similar dependence of surface roughness on feed was found in earlier studies [8, 11, 12, 18, 31]. The results differ slightly because different cutting tools/inserts are used, but the trends are very similar. As the feed increases, the cutting forces increase, which contributes to higher flank wear. The intensification of flank wear contributes to an increase in waviness and a deterioration in cylindricity, which in turn leads to an increase in dimensional deviation. A larger feed creates wider valleys on the workpiece, which contributes to an increase in surface roughness.

As the corner radius increases, flank wear decreases. As the corner radius increases, the length of the cutting edge in contact with the workpiece increases, dissipating heat from the longer cutting edge and reducing flank wear. Several researchers were studying the connection between surface roughness and the corner radius. In previous studies, it was found that the surface roughness can decrease [12, 31] or increase [8] with an increase in the corner radius. In this study, as the corner radius increases, the dimensional deviation and surface roughness initially decrease and then increase slightly. Larger corner radii produce smaller peaks on the surface of the workpiece and at the same time less waviness. Therefore, a reduction in dimensional deviation and surface roughness up to a certain corner radius value can occur. After reaching this critical corner radius value, small vibrations obviously occur, which have an effect on the deterioration of the dimensional deviation and surface roughness, with the exception of flank wear.

The flank wear decreases slightly with increasing depth of cut, similar to [30]. As the depth of cut increases, greater forces are required to break and remove the chips. As a result, the strength of the cutting edge decreases and flank wear increases. Higher flank wear contributes to an increase in dimensional deviation.

Wiper inserts improve surface roughness, which is consistent with the results of an earlier study [8]. Wiper inserts are designed with a larger number of wipers and therefore contribute to a significant reduction in surface roughness. In addition, wiper inserts have a longer cutting edge so that they wear more slowly, i.e. the use of wiper inserts reduces flank wear.

The optimisation results (Table 9) show that it is always advantageous to turn C45 steel with wiper inserts and with a corner radius r = 1.2 mm, regardless of the weights of the output parameters. This is due to the fact that these two input parameters have no influence on the *MRR* and have a positive effect on ΔD, *VB* and *Ra*.

In the first case (Table 8), where all output parameters are given the same importance ($w_{\Delta D}$=w_{VB}=w_{Ra}=w_{MMR}=1), the cutting speed was close to the average level (v_c=340 mm/min), the depth of cut was at the maximum level (a_p=3 mm) and the feed was close to the average level (f=0.2 mm/rev). Increasing the depth of cut had a positive effect on *MRR* and the least negative effect on ΔD, *Ra* and *VB*. Increasing the cutting speed and feed had a positive effect on *MRR* and a negative effect on ΔD, *Ra* and *VB*. The negative influence

of cutting speed and feed was compensated by the corner radius r=1.2 mm and the wiper insert, which resulted in the best values for ΔD and *Ra* and almost the best values for *VB*.

In the second case shown in Table 8, where equal importance was given to ΔD, *Ra* and *MRR* ($w_{\Delta D}=w_{Ra}=w_{MMR}=1$) and no importance was given to *VB* ($w_{VB}=0$), the cutting speed was at the maximum level (v_c=400 mm/min), the depth of cut was at the maximum level (a_p=3 mm) and the feed was at the maximum level (f=0.25 mm/rev). This is due to the fact that the *MRR* is highest when the cutting speed, depth of cut and feed are at their maximum. In addition, the negative influence of these three parameters on ΔD and *Ra* was compensated with a corner radius of r=1.2 mm and a wiper insert, and the best values for ΔD and *Ra* were achieved.

In the third case of Table 8, where equal importance was given to ΔD and *Ra* ($w_{\Delta D}=w_{Ra}=1$) and no importance was given to *VB* and *MRR* ($w_{VB}=w_{MMR}=0$), the cutting speed was close to the minimum value (v_c=328 mm/min), the depth of cut was close to the minimum value (a_p=2.1 mm) and the feed was at the minimum value (f=0.1 mm/rev). This is due to the fact that ΔD and *Ra* decrease with a reduction in cutting speed, depth of cut and feed.

5. CONCLUSION

In this study, a scientific approach has been proposed and proven that allows the process of dry turning of C45 steel for defined input parameters to be comprehensively evaluated, modelled and optimised based on the results of experimentation, statistical analysis, modelling, optimisation and confirmation.

For different combinations of input parameters, the values of the output parameters vary over wide ranges, namely:

- ΔD in the range of 0.014–0.291 mm and with a ratio of 20.79,
- *VB* in the range of 0.084–0.213 mm and with a ratio of 2.54,
- *Ra* in the range of 0.172–7.237 μm and with a ratio of 42.08,
- *MRR* in the range of 60–300 mm^3/min and with a ratio of 5.

This shows that it is possible to optimise the dry turning of C45 steel for various reasons in order to achieve the required quality characteristics, which is very important with regard to the possibility of practical application of the developed methodology.

The most influential input parameters on ΔD are feed and corner radius, while cutting speed, insert type and depth of cut had a slightly smaller influence. The most influential parameters on *VB* are cutting speed, corner radius and insert type, while feed and depth of cut have a slightly lower influence. The parameters with the greatest influence on *Ra* are feed, corner radius and insert type. The parameters influencing *MRR* are cutting speed, feed and depth of cut.

The optimal combinations of input parameters vary with the requirements for the defined importance of the output parameters. Different combinations of optimal input parameters resulted from the different importance (weighting coefficients) of the output parameters. The results obtained show that dry turning with corner radius of r=1.2 mm and a wiper insert is suitable to be performed independently of other production requirements. The percentage optimisation errors were in the range of 1.01-6.25 % for ΔD, in the range of 1.27-3.10 % for *VB* and in the range of 1.31-2.15 % for *Ra*. These percentage errors correspond to absolute errors in the range of 0.001-0.002 mm for ΔD, in the range of 0.002-

0.004 for *VB* and in the range of 0.003-0.018 μm for *Ra*. The values of the percentage errors and especially the absolute errors show the possibility of practical implementation of the developed models in a real production environment.

The limitations of the applied methodology are reflected in the fact that the models are applicable under the conditions under which the experiments were conducted. Therefore, it is planned to consider a larger number of input parameters as well as wider ranges and additional input parameters in future research.

Acknowledgement: *This research has been supported by the Ministry of Science, Technological Development and Innovation (Contract No. 451-03-65/2024-03/200156), the Faculty of Technical Sciences, University of Novi Sad through project "Scientific and Artistic Research Work of Researchers in Teaching and Associate Positions at the Faculty of Technical Sciences, University of Novi Sad" (No. 01-3394/1) and the University of Slavonski Brod (project "SmartPRO-Modelling of Processes for Smart Manufacturing").*

REFERENCES

1. Jovicic, G., Milosevic, A., Kanovic, Z., Sokac, M., Simunovic, G., Savkovic, B., Vukelic, D., 2023, *Optimization of Dry Turning of Inconel 601 Alloy Based on Surface Roughness, Tool Wear, and Material Removal Rate*, Metals, 13(6), 1068.
2. Vukelic, D., Simunovic, K., Kanovic, Z., Saric, T., Tadic, B., Simunovic, G., 2021, *Multi-objective optimization of steel AISI 1040 dry turning using genetic algorithm*, Neural Computing and Applications, 33(19), pp. 12445-12475.
3. Jozić S., Dumanić I., Bajić D., 2020, *Experimental analysis and optimization of the controllable parameters in turning of en aw-2011 alloy; dry machining and alternative cooling techniques*, Facta Universitatis-Series Mechanical Engineering, 18(1), pp. 13-29.
4. Vukelic, D., Prica, M., Ivanov, V., Jovicic, G., Budak, I., Luzanin, O., 2022, *Optimization of surface roughness based on turning parameters and insert geometry*, International Journal of Simulation Modelling, 21(3), pp. 417-428.
5. Guvenc, M.A., Bilgic, H.H., Mistikoglu, S., 2023, *Identification of chatter vibrations and active vibration control by using the sliding mode controller on dry turning of titanium alloy (Ti6Al4V)*, Facta Universitatis-Series Mechanical Engineering, 21 (2), pp. 307-322.
6. Grzesik, W., 2006, *Composite layer-based analytical models for tool-chip interface temperatures in machining medium carbon steels with multi-layer coated cutting tools*, Journal of Materials Processing Technology, 176(1-3), pp. 102-110.
7. Piska, M., Polzer, A., Cihlarova, P., Stankova, D., 2009, *On the structural integrity of the nano-PVD coatings applied on cutting tools*, Damage and Fracture Mechanics: Failure Analysis of Engineering Materials and Structures, pp. 195-204.
8. Stachurski, W., Kruszyński, B., Midera, S., 2012, *Influence of cutting conditions in turning with wiper type inserts on surface roughness and cutting forces*, Mechanics and Mechanical Engineering, 16(1), pp. 25-32.
9. Nieslony, P., Grzesik, W., Laskowski, P., Habrat W., 2013, *FEM-Based modelling of the influence of thermophysical properties of work and cutting tool materials on the process performance*, Procedia CIRP, 8, pp. 3-8.
10. Segreto, T., Simeone, A., Teti, R., 2014, *Principal component analysis for feature extraction and NN pattern recognition in sensor monitoring of chip form during turning*, CIRP Journal of Manufacturing Science and Technology, 7(3), pp. 202-209.
11. Michal, P., Vagaská, A., Gombár, M., Kmec, J., 2014, *Mathematical modelling and optimization of technological process using design of experiments methodology*, Applied Mechanics and Materials, 616, pp. 61-68.
12. Selvam, M.D., Senthil, P., 2016, *Investigation on the effect of turning operation on surface roughness of hardened C45 carbon steel*, Australian Journal of Mechanical Engineering, 14(2), pp. 131-137.
13. Horvath, R., Lukacs, J., 2017, *Application of a force model adapted for the precise turning of various metallic materials*, Strojniski Vestnik-Journal of Mechanical Engineering, 63(9), pp. 489-500.
14. Necpal, M., Pokorný, P., Kuruc, M., 2017, *Finite element analysis of tool stresses, temperature and prediction of cutting forces in turning process*, Solid State Phenomena, 261, pp. 354-361.
15. Vereschaka, A.A., Grigoriev, S.N., Sitnikov, N.N., Batako, A.D., 2017, *Delamination and longitudinal cracking in multi-layered composite nano-structured coatings and their influence on cutting tool life*, Wear, 390-391, pp. 209-219.

16. Vereschaka, A.A., Bublikov, J.I., Sitnikov, N.N., Oganyan, G.V., Sotova, C.S., 2018, *Influence of nanolayer thickness on the performance properties of multilayer composite nano-structured modified coatings for metal-cutting tools*, International Journal of Advanced Manufacturing Technology, 95(5-8), pp. 2625-2640.
17. Klocke, F., Lortz, W., Trauth, D., 2018, *Analysis of the dynamic chip formation process in turning*, International Journal of Mechanical Sciences, 135, pp. 313-324.
18. Dragicevic, M., Begović, E., Peko, I., 2019, *Optimization of dry turning process parameters using Taguchi method combined with fuzzy logic approach*, Proceedings on Engineering Sciences, 1(1), pp. 429-435.
19. Gjelaj, A., Berisha, B., Smaili, F., 2019, *Optimization of turning process and cutting force using multiobjective genetic algorithm*, Universal Journal of Mechanical Engineering, 7(2), pp. 64-70.
20. Zmarzły, P., 2020, *Technological heredity of the turning process*, Tehnicki vjesnik-Technical Gazette, 27(4), pp. 1194-1203.
21. Zajac, J., Duplak, J., Duplakova, D., Cizmar, P., Olexa, I., Bittner, A., 2020, *Prediction of cutting material durability by T = f(vc) dependence for turning processes*, Processes, 8(7), 789.
22. Usman, M.M., Zou, P., Tian, Y., Wang, W., 2020, *Experimental investigation on surface functional indices in Ultrasonic Elliptical Vibration Cutting of C45 carbon steel*, International Journal of Advanced Manufacturing Technology, 109(1-2), pp. 187-200.
23. Mikołajczyk, T., Latos, H., Pimenov, D.Y., Paczkowski, T., Gupta, M.K., Krolczyk, G., 2020, *Influence of the main cutting edge angle value on minimum uncut chip thickness during turning of C45 steel*, Journal of Manufacturing Processes, 57, pp. 354-362.
24. Titu, A.M., Pop, A.B., Sandu, I.G., 2021, *Study of temperature and stresses using finite element analysis in turning of C45 material*, Journal of Physics: Conference Series, 1960(1), 012023.
25. Oleksik, M., Dobrotă, D., Tomescu, M., Petrescu, V., 2021, *Improving the performance of steel machining processes through cutting by vibration control*, Materials, 14(19), 5712.
26. Abidi, Y., 2021, *Analysis of the compromise between cutting tool life, productivity and roughness during turning of C45 hardened steel*, Production Engineering Archives, 27(1), pp. 30-35.
27. Zaida, H., Bouchelaghem, A.M., Chehaidia, S.E., 2021, *Experimental study of tool wear evolution during turning operation based on DWT and RMS*, Defect and Diffusion Forum, 406, pp. 392-405.
28. Ivchenko, O., Ivanov, V., Trojanowska, J., Zhyhylii, D., Ciszak, O., Zaloha, O., Pavlenko, I., Hladyshev, D., 2022, *Method for an Effective Selection of Tools and Cutting Conditions during Precise Turning of Non-Alloy Quality Steel C45*, Materials, 15(2), 505.
29. Kovalčík, J., Mašek, P., Malý, J., Kožmín, P., Syrovátka, J., 2022, The Effect of Coatings on Cutting Force in Turning of C45 Steel, Materials, 15(2), 590.
30. Jurko, J., Miškiv-Pavlík, M., Hladký, V., Lazorík, P., Michalík, P., Petruška, I., 2022, *Measurement of the Machined Surface Diameter by a Laser Triangulation Sensor and Optimalization of Turning Conditions Based on the Diameter Deviation and Tool Wear by GRA and ANOVA*, Applied Sciences, 12(10), 5266.
31. Vukelic, D., Simunovic, K., Kanovic, Z., Saric, T., Doroslovacki, K., Prica, M., Simunovic, G., 2022, *Modelling surface roughness in finish turning as a function of cutting tool geometry using the response surface method, Gaussian process regression and decision tree regression*, Advances in Production Engineering and Management, 17(3), pp. 367-380.
32. Niemczewska-Wojcik, M., Madej, M., Kowalczyk, J., Piotrowska, K., 2022, *A comparative study of the surface topography in dry and wet turning using the confocal and interferometric modes*, Measurement, 204, 112144.
33. Kuruc, M., Vopát, T., Peterka, J., Necpal, M., Šimna, V., Milde, J., Jurina, F., 2022, *The Influence of Cutting Parameters on Plastic Deformation and Chip Compression during the Turning of C45 Medium Carbon Steel and 62SiMnCr4 Tool Steel*, Materials, 15(2), 585.
34. Moravčíková, J., Moravčík, R., Palcut, M., 2022, *Effect of Heat Treatment on the Resulting Dimensional Characteristics of the C45 Carbon Steel after Turning*, Metals, 12(11), 1899.
35. Slusarczyk, L., Franczyk, E., 2023, *Analytical method for determining cutting forces during orthogonal turning of C45 steel*, Materials Research Proceedings, 28, pp. 1313-1322.